

“coarse” to “fine” in terms of the spatial scale of the stimulus, and from higher to lower visual areas in terms of the anatomical visual hierarchy (Hochstein & Ahissar, 2002; Murray et al., 2002).

The model proposes that, initially, the physical parts of the stimulus (i.e., the inducing elements) are processed in a feedforward direction in order to generate a rough hypothesis of a “salient region” in the LOC (Stanley & Rubin, 2003, 2005), or in dorsal stream regions to demarcate an object’s location in space (Murray et al., 2002). This idea is consistent with electrophysiological studies in humans reporting the earliest (in time) sensitivity to illusory stimuli in the LOC (Yoshino et al., 2006; Murray et al., 2002, 2004; Halgren, Mendola, Chong, & Dale, 2003). In addition, the model assumes that V1 neurons, which are driven by the inducers, simultaneously excite neighboring neurons with a similar orientation preference via horizontal connections (Pillow & Rubin, 2001). Subsequently, feedback signals re-enter V1 in order to guide the signal cascade. There are electrophysiological data from the awake monkey showing that illusory contour responses in V1 only occurred 40 msec after responses in V2 have been observed (Lee & Nguyen, 2001), which indicates that the activity in V1 was amplified by feedback signals. The generation of feedback signals might occur automatically (Hupe et al., 1998). We make the additional assumption that they can vary in strength and with respect to their predominant target population, depending on the perceptual requirements of the task (see the Reverse Hierarchy Theory, Ahissar & Hochstein, 2004; Hochstein & Ahissar, 2002; or the high-resolution buffer hypothesis, Lee, 2003, for closely related concepts). This idea dates back to the psychoanatomic matching logic (Julesz, 1971) and simply states that a stimulus will be processed by those neurons which are best equipped to process it with respect to their firing preferences. When demands for spatial resolution are high (e.g., when trying to thread a needle), neurons with small receptive fields seem better suited to represent fine differences than neurons with larger receptive fields. In contrast, when fine differences are less emphasized (e.g., when searching for a familiar face in a crowd), neurons that pool different aspects of information from different parts of the visual field seem better suited than spatially restricted neurons.

If observers have to discriminate differences in the curvature of an illusory contour, the illusory contour has to be represented by neurons which map differences in curvature to different activity patterns. V1 neurons seem to be the best candidate for this type of cortical representation because they have the smallest receptive field size (e.g., see Smith et al., 2001 for receptive field size estimates in humans). In support of this view, we observed an increased activation in V1 when subjects learned to discriminate between illusory contours of different curvature (similar to the stimuli

used here; Maertens & Pollmann, 2005). In contrast, neurons in the LOC are rather unlikely to respond differentially to illusory contours of different curvature because they would all fall in the same large receptive field and the differences would be lost. We therefore suggest that V1 neurons are of critical importance when a neural representation of different illusory contour curvatures has to be formed. We also suggest that this neural representation in V1 is the basis for our corresponding percepts of a crisp illusory bounding contour. If this is true, performance in a task that requires the perception of a crisp illusory contour should be impaired when one disrupts the representation of that illusory contour in V1.

To experimentally address this question, we adopted a task which required observers to discriminate the curvature of one of the bounding illusory contours of slightly deformed Kanizsa-type illusory shapes (Ringach & Shapley, 1996). Previous studies have shown that good performance on this task depends on the ability to perceive illusory contours (Gold, Murray, Bennett, & Sekuler, 2000; Rubin, Nakayama, & Shapley, 1997; Ringach & Shapley, 1996). As a method for interfering with the cortical representation of the illusory contour, we positioned the inducing elements of a Kanizsa square so that a large portion of the illusory contour critical to the task fell in the region of the visual field corresponding to the “blind spot.”

The “blind spot” results from a retinal nonuniformity where the optic nerve exits the eye, which is called the optic disc (e.g., Komatsu, Kinoshita, & Murakami, 2002). The human optic disc has a diameter of about 2 mm on the retina, corresponding to a diameter of 5° to 6° in terms of visual angle in the visual field. It is located in the nasal part of the retina with its inner edge being approximately 15° away from and 2–3° below the foveal center. As a consequence of the gap in the photoreceptor array, no information is conveyed from this part of the visual field to the consecutive stages of visual information processing, which is why it is called “blind.” In histological preparations of macaque (Tootell, Switkes, Silverman, & Hamilton, 1988) and human V1 (Horton, Dagi, McCrane, & DeMonasterio, 1990), the blind spot can be identified in the input layer IV as an elliptical *monocular* region, about four ocular dominance columns wide. Functionally, V1 neurons within the retinotopic representation of the blind spot (referred to as “blind spot representation” from now on) are driven entirely by the ipsilateral eye (Awater, Kerlin, Evans, & Tong, 2005; Tong & Engel, 2001). Results from a functional magnetic resonance imaging study in humans suggest that the cortical blind spot representation is confined to visual area V1 (Awater et al., 2005; Tootell et al., 1998) and lost later on. Most of the time we are completely unaware of this circumscribed blind region. It is restricted to monocular viewing, and our visual system compensates for the loss

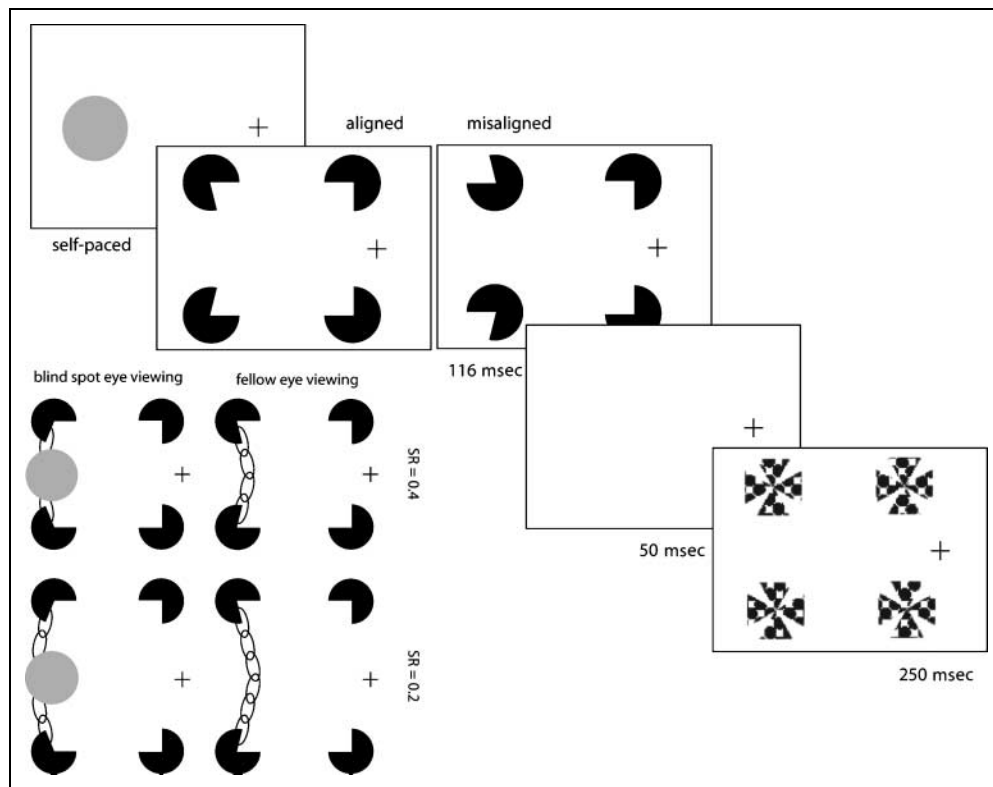
of information by actively filling in the missing part of the visual field (Ramachandran, 1992a) with information from the surround.

We formulated the following hypotheses: If V1 neurons are required to represent a fine-grained illusory contour, then curvature discrimination that operates on this representation should be severely impaired when the illusory contour traverses the blind spot. Alternatively, if curvature discrimination is based on illusory contour representations in higher visual cortical areas, discrimination performance should be identical for illusory contours which traverse the blind spot and those that do not. Based on the evidence that ocular dominance is lost after V1 and replaced by neurons which receive input from both eyes (Ts'o, Frostig, Lieke, & Grinvald, 1990; Tootell & Hamilton, 1989), the blind spot should not interfere with illusory contour representations in these binocular representations.

To test the above hypotheses, we presented a square-like Kanizsa figure to one side of fixation positioned so that its lateral illusory contour traversed the region of the visual field corresponding to the blind spot of the eye ipsilateral to the stimulus. Curvature discrimination thresholds for the lateral illusory contour were compared between the ipsilateral (blind spot) eye and the contralateral (control) eye. We also varied the support ratio (SR) (i.e., the ratio between the luminance-defined part of an illusory contour and its total side length), which has been shown to influence the clarity of illusory contour perception (Stanley, & Rubin, 2003;

Ringach, & Shapley, 1996; Shipley & Kellman, 1992). For illusory contours presented away from the blind spot, we expected finer discrimination thresholds with increasing SR. A larger support of the illusory contour would allow a more accurate illusory contour representation, which might in turn improve the accuracy of the curvature discrimination. In contrast, for illusory contours traversing the blind spot, we predicted a selective impairment in illusory curvature discrimination performance at the largest SR (i.e., smallest distance between inducers). This prediction is counterintuitive but based on the idea that inducers which are almost adjacent to the blind spot cannot propagate the intracortical signal spread (Figure 1). It has been reported that long-range intrinsic connections preferentially connect monocular regions of same-eye ocular dominance columns (Malach, Amir, Harel, & Grinvald, 1993). Because the cortical blind spot representation exclusively contains ocular dominance columns from the ipsilateral eye, there are no targets for signals propagated by neurons excited by the pacmen which are presented to the contralateral eye. The amount of interference with the illusory contour representation caused by the blind spot should be largest for the largest SR (smallest inducer distance) and least for the smallest SR. In the latter case, the larger inducer distance might allow a residual contour representation to build up around the blind spot. We predict that the lack of an illusory contour representation in V1 should result in poor curvature discrimination performance.

Figure 1. Schematic sequence of events in one experimental trial. Inset depicts the smallest (upper panels) and the largest (lower panels) SRs for the blind spot (left column) and the fellow eye (right eye). The ellipses represent receptive fields of the neurons in V1 that are supposed to be involved in the generation of an illusory contour representation. The gray circle represents the region corresponding to the blind spot. For the large SR, the inducers almost directly abut the blind spot and leave hardly any room for a representation of the illusory contour.



METHODS

Participants

Four female observers (including one of the authors, M. M.) with a mean age of 24 years ($SD = 2.7$ years) participated in the experiment. The other three observers were students of the University of Magdeburg. They participated to fulfill a course requirement. All observers were right-handed and had normal or corrected-to-normal vision.

Stimuli

Stimulus delivery and response registration were controlled by Presentation software (Version 9.51, <http://nbs.neuro-bs.com>). Stimuli were presented on a 390 × 290 mm screen with a resolution of 1280 × 1024 pixel and a refresh rate of 60 Hz. Participants sat in a dimly lit room. Viewing was monocular at an individually optimized distance of about 80 cm (see below), with either the left (blind spot condition) or the right eye (non-blind-spot condition) occluded with an eye patch. A chin and forehead rest was used to minimize head movements.

Illusory shapes were distorted Kanizsa squares consisting of four white inducers (pacmen) that were aligned to induce the illusion of a figure in front of four disks. The inducers' diameter subtended 3.6° visual angle. To optimally align the stimulus within the screen, the fixation mark was displaced by 4.6° visual angle to the left of the screen center (Figure 1). All participants were tested with their right eye as the blind spot eye. The horizontal distance between the fixation cross and the closest inducers' center was 6° visual angle. The horizontal distance between inducers' centers was 12°. This configuration allowed the most peripheral vertical illusory edge to be confined to the eccentricity of the blind spot region (~15°).

The inducers which were close to fixation had constant openings of 90° so as not to convey any information about curvature or local angle. The openings of the peripheral inducers were either smaller than 90°, resulting in outward curvature (convex); or larger than 90°, creating inward curvature (concave, Figure 1). In the control condition (see Design), the inducing elements were misaligned. Everything else being equal, the peripheral inducer openings were facing outwards and therefore did not give rise to an illusory shape. The amount of the angular opening varied in steps of two between 10° and 20° in both directions ($\pm 90^\circ$).

The vertical distance between the inducers varied according to the SR and corresponded to 8.6°, 11.4°, and 14.3° visual angle. Stimuli were masked backwards by four white pinwheel shapes consisting of eight (four checkerboard-patterned and four black) sectors of 45° presented at the positions of the inducers (see Figure 1). To determine the individual blind spot locations of each

participant, in terms of the appropriate viewing distance, a white disk with a diameter of 4.3°, centered at about 15° visual angle to the right side of fixation, was presented at the beginning of each trial. The observers adjusted their position until the white disk disappeared when fixation was stable. Participants were instructed to start a trial only if the white disk had completely disappeared. Immediately after the trial had been initiated by the observer, the Kanizsa stimulus was presented for 116 msec followed after a blank interval of 50 msec by the mask shown for 250 msec (Figure 1). The rapid presentation should assure that the outer edge of the Kanizsa square fell into the blind spot region of the right eye. The limited exposure duration makes it unlikely that voluntary eye movements have been carried out, and even if subjects did engage in saccades, we think it is unlikely that they have a differential effect on the experimental conditions to explain (part of) the observed pattern of results.

Design

We implemented a 2 × 3 × 2 design with the factors eye (blind-spot vs. control), SR (small, medium, large), and task (curvature vs. local orientation discrimination). Tripathy, Levi, and Ogmen (1996) have shown that a comparison between eyes, but within one visual hemifield and cortical hemisphere, is the more appropriate control condition relative to a within-eye comparison between the blind spot region and an isoeccentric region in the opposite hemifield. Their results suggest that comparable performance levels are obtained when stimuli are presented to corresponding cortical loci rather than to corresponding eccentricities in the two hemiretinas. The SR was manipulated by using three different interinducer distances (see Stimuli), yielding SRs of 0.25, 0.3, and 0.4.

We introduced a local orientation discrimination task, referred to as the local task, to control for the possibility that participants would engage in a different strategy to solve the task. The pacmen were rotated so that their mouths were facing outward, and thus, would not induce an illusory contour. Participants were asked to discriminate the stimuli on the basis of the local information conveyed by the orientation of the vertical pacmen edge (Figure 1). If participants relied exclusively on the local information of the inducers independent of their alignment, and thus, independent of the presence or absence of a contour percept, identical discrimination performance should be observed in both tasks. The interinducer distance was varied for the misaligned (outward facing) pacmen in the same way as for the aligned pacmen.

The difficulty of the task was manipulated by varying α , the deviation of the openings of the angular inducers from 90°. The deviation α was the independent variable and was varied following the method of constant stimuli.

This allowed us to average the performance of different observers to obtain a single psychometric function. We measured participants' monocular curvature discrimination thresholds for illusory contours, and their monocular local orientation discrimination thresholds using a two-alternative forced-choice method of constant stimuli.

Procedure

Data were collected in four sessions that were completed within a period of maximally 2 weeks. Participants were extensively trained on the tasks before data collection started. They performed two to four sessions analogous to the testing session. Three participants ran through a blocked task sequence with only one of the tasks being performed in each session. The order of task execution followed an ABBA scheme, with two participants starting with the illusory curvature discrimination and the third starting with the local discrimination task. These three participants were explicitly instructed as to which task they were performing in each session. In the misaligned conditions, they were instructed to discriminate the orientation of the vertical edge of one of the outer pacmen. In the illusory contour condition, observers were asked to discriminate between leftward (concave) and rightward (convex) curvature. Observers indicated direction of curvature or orientation by pressing the left or the right mouse button correspondingly. They were instructed to make as few errors as possible. For the fourth subject (M. M.), the task order was randomized within experimental sessions and blocks. In the absence of the possibility to build up a "task set" and to endogenously attend to either the illusory curvature or the local information, M. M.'s discrimination performance was determined exclusively by the stimulus.

The factor eye was blocked within sessions following an AB-BA-AB-BA scheme over the four sessions (hyphens separate sessions), with half the participants starting with the blind spot (right) eye, and the other half with the non-blind-spot (left) eye. For those participants with the blocked task factor, the factor eye was nested within task. The interinducer distance, as well as the angle of the openings, varied randomly within experimental blocks. One experimental session was composed of six experimental blocks, three for each eye. One block comprised 360 trials, 120 trials for each of the SRs. Half of the trials of each SR ($n = 60$) contained inducers with openings that were larger than 90° , and they were equally distributed with respect to the inducer openings. Thus, after four sessions, 20 observations were available for each stimulus level in each condition.

In order to fit the psychometric functions and to derive threshold and slope estimates, we computed the fraction of "convex" responses in each condition

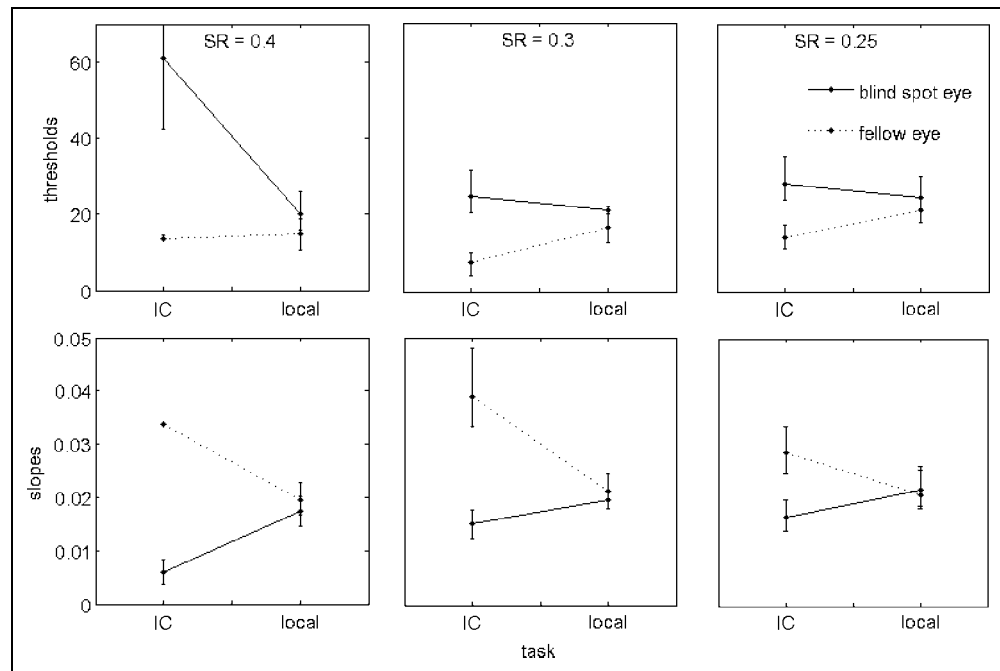
as a function of the amount of the inducer opening ($\alpha = -20^\circ, -18^\circ, \dots, -10^\circ, 10^\circ, 12^\circ, \dots, 20^\circ$). We did this for each individual observer ($k = 20$ observations per data point) and also for the average performance of all four subjects ($k = 80$). Responses were fit with a four-parametric logistic psychometric function $\Psi(x) = g + (1 - g - l) * 1/(1 + \exp(-((x - a)/b)))$ using Psignifit, version 2.5.6 (a software package which implements the maximum likelihood method, Wichmann & Hill, 2001b; and see <http://bootstrap-software.org/psignifit/>). The parameters a and b determine the horizontal displacement of the curve and its slope, respectively. The value of g corresponds to the predicted performance in the absence of a stimulus (in the case of two alternatives like in the current experiment, it is usually <0.5), and in the current experiment its maximum value was 0.05. Parameter l accounts for stimulus-independent errors (e.g., response lapses) with $(1 - l)$ corresponding to the predicted performance with an arbitrarily large stimulus. In the current experiment, the maximum l was 0.05 because it is assumed that observers do not make stimulus-independent errors at high rates. We calculated the 80% performance thresholds ($\Psi(x) = .8$) and the slopes at $\Psi(x) = 0.5$. Confidence intervals (1 *SD*) for thresholds and slopes were calculated using a bias-corrected and accelerated (BCa) bootstrap parametric method implemented by Psignifit for each psychometric function on the basis of 2000 simulations (Wichmann & Hill, 2001a).

RESULTS

Accuracy

Figure 2 shows the performance thresholds for the group responses for both eyes and both tasks. Thresholds in the curvature discrimination task are interpreted as the amount of curvature an observer needed to respond correctly in 80% of the trials. The results show a marked impairment for curvature discrimination of illusory contours presented to the blind spot eye compared to those presented to the fellow eye (Figure 2). This impairment is most pronounced in the largest SR condition in which most part of the illusory contour is confined to the blind spot region. In contrast, thresholds did not significantly differ between the tasks for the same SR when the stimulus was viewed with the control eye. Performance also did not differ between the eyes for the local task. A much higher and statistically significant difference in discrimination thresholds was obtained, however, for illusory contours presented to the blind spot eye. The corresponding threshold estimate was far outside the 95% confidence limits obtained for the other threshold estimates, and its own confidence interval excludes the other three threshold estimates. This selective increase in threshold was observed in all four subjects. A slightly modified interaction pattern

Figure 2. Parameter estimates derived from fitting psychometric functions $\Psi(x)$ to the averaged results of four observers. Top: 80% performance thresholds; Bottom: slopes derived at $\Psi(x) = 0.5$. Parameter estimates are depicted as a function of the task (x-axis), the eye of viewing (panel variable), and the SR (columns). The error bars indicate the 95% confidence intervals of the parameter estimates and were derived using parametric bootstrap resampling for 2000 samples. IC = illusory curvature discrimination; LC = local discrimination.



was observed for the medium and the smallest SRs. Although curvature discrimination thresholds significantly differed between the eyes, no eye difference was observed for local discrimination performance. The interaction between the factors eye and task is attributable to the fact that for the fellow eye, curvature discrimination significantly outperformed local discrimination performance. An advantage for illusory curvature over local discrimination with the control eye was observed in all subjects. The effect was also evident for the smallest SR, but only in three out of four subjects, which is why the group threshold estimates did not significantly differ. Finally, no significant main effect of the SR was observed.

The result pattern for the slope estimates, a measure indicating the sensitivity (or reliability) of the observer to discriminate between two alternatives, parallels the

pattern observed for the thresholds (Figure 2) with one exception. For the largest SR, differences in illusory contour curvature can be discriminated much more reliably than differences in local orientation when the fellow eye is used (Figure 2, lower left panel).

To test the statistical significance of the observed effects in individual observers, we performed three-way analyses of variance (ANOVAs) and follow-up *t* tests upon the individual relative frequencies of correct responses (Table 1). Overall, 20 observations were available for each participant (frequency of correct responses averaged over the 12 levels of α), and we treated those as being independently sampled from each combination of the factor levels. Each of the four ANOVAs yielded a significant main effect for the factor eye and a significant interaction between the task and the eye (see Table 2). In all four subjects, the significant effect of the factor

Table 1. Mean Fraction of Correct Responses Averaged over Inducer Angle α for Individual Subjects, Separated for Eye, Support Ratio (SR), and Task

	<i>Blind Spot Eye</i>								<i>Fellow Eye</i>							
	<i>SR = 0.4</i>		<i>SR = 0.3</i>		<i>SR = 0.25</i>		<i>Mean</i>		<i>SR = 0.4</i>		<i>SR = 0.3</i>		<i>SR = 0.25</i>		<i>Mean</i>	
	<i>IC</i>	<i>LC</i>	<i>IC</i>	<i>LC</i>	<i>IC</i>	<i>LC</i>	<i>IC</i>	<i>LC</i>	<i>IC</i>	<i>LC</i>	<i>IC</i>	<i>LC</i>	<i>IC</i>	<i>LC</i>	<i>IC</i>	<i>LC</i>
M. M.	0.63	0.76	0.74	0.77	0.75	0.71	0.70	0.75	0.93	0.78	0.98	0.77	0.96	0.76	0.96	0.77
#1	0.54	0.69	0.75	0.75	0.70	0.79	0.66	0.74	0.85	0.73	0.90	0.80	0.80	0.75	0.85	0.76
#2	0.56	0.60	0.58	0.59	0.58	0.69	0.57	0.68	0.67	0.64	0.70	0.63	0.67	0.65	0.63	0.64
#3	0.61	0.83	0.75	0.83	0.78	0.79	0.71	0.82	0.90	0.83	0.93	0.87	0.88	0.83	0.90	0.84

IC = illusory curvature discrimination; LC = local orientation discrimination.

Table 2. Results of Individual Three-way ANOVAs on Fraction of Correct Responses

	<i>Task</i>		<i>Eye</i>		<i>SR</i>		<i>Task × Eye</i>		<i>Task × SR</i>		<i>Eye × SR</i>		<i>Task × Eye × SR</i>	
	<i>F</i>	<i>p</i>	<i>F</i>	<i>p</i>	<i>F</i>	<i>p</i>	<i>F</i>	<i>p</i>	<i>F</i>	<i>p</i>	<i>F</i>	<i>p</i>	<i>F</i>	<i>p</i>
M. M.	27.74	<.001	94.84	<.001			68.03	<.001	5.14	.006				
#1			39.98	<.001	11.62	<.001	27.08	<.001			7.21	<.001		
#2			10.39	.001			5.71	.018						
#3			46.99	<.001	3.39	.035	26.77	<.001	3.50	.032			5.09	.007

“eye” resulted from a larger fraction of correct responses for the fellow (mean $f = 0.8$) than for the blind spot eye [mean $f = 0.7$; $t_{\min}(238) = 3.20$, $p = .002$]. In order to further explore the interaction between task and eye, we performed t tests to compare the performance between the eyes separately for both tasks. Significantly better performance for the fellow (mean $f = 0.84$) than for the blind spot eye (mean $f = 0.66$) was observed for the illusory curvature discrimination task for all four subjects [$t_{\min}(118) = 4.0$, $p < .001$]. The same t test was performed for the local discrimination task, but for none of the subjects was a significant difference between the eyes observed ($p_{\min} = .2$, mean $f = 0.75$ for both eyes). As can be inferred from Figure 3, these effects were most pronounced for the largest SR. However, probably due to a lack of statistical power, the three-way interaction between task, eye, and SR was not statistically significant. There is a feature about the results which is conveyed differently by the mean proportion of correct responses and the mean threshold estimates. The mean performance thresholds for the largest SR (Figure 2) imply a selective impairment in the illusory curvature discrimination task when performed with the blind spot eye. The same is true for the fraction of correct responses, but in addition, they indicate that there was a benefit for the illusory curvature

task when performed with the fellow eye (Figure 3). This discrepancy between fraction correct responses and thresholds results from the steeper slope in this condition (Figure 2, lower panel). Although the threshold remained unchanged, a higher number of correct responses would be reflected in a higher slope, which is exactly what we observed.

Response Latencies

Although participants were instructed to focus on accuracy rather than on speed, we explored whether the experimental manipulations also affected response latencies. Figure 4 shows the group mean reaction times averaged over alphas for each experimental condition. The experimental manipulations had distinct effects on the reaction times as well, and their pattern paralleled that obtained for the accuracy measures. The most prominent effect is the interaction between task and eye. At all SRs, shorter response times were observed for local than for illusory curvature discrimination when the blind spot eye was used, whereas the opposite was true when stimuli were viewed with the fellow eye (Figure 4). The average response time pattern was evident in the individual result patterns as well. Three-way ANOVAs performed on individual mean response

Figure 3. Mean fraction of correct responses averaged across observers and levels of the inducer angle α as a function of the SR, the experimental task, and the eye of viewing. The different SRs are depicted in the different panels and decrease from left to right. The tasks are plotted on the axis: IC = illusory curvature discrimination; LC = local discrimination. Error bars indicate 2 standard errors of the mean derived by nonparametric bootstrap resampling with $n = 2000$ samples.

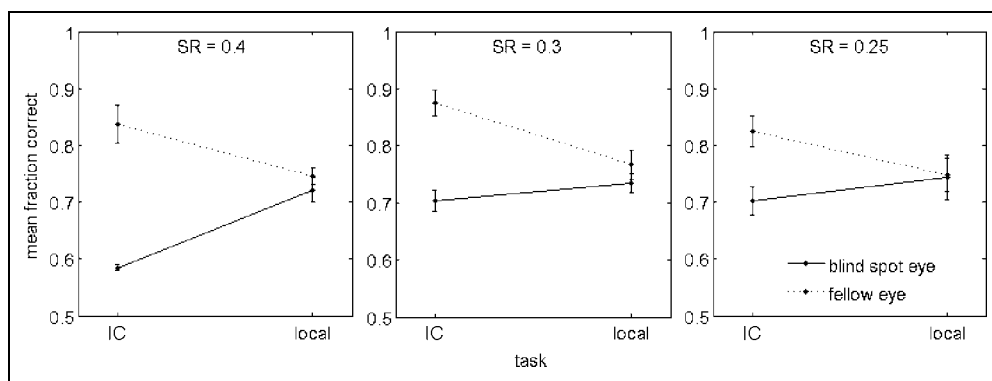
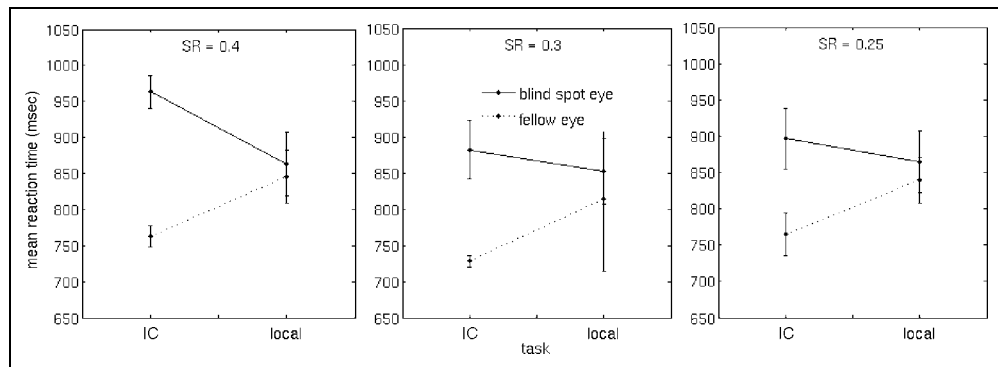


Figure 4. Mean response latencies averaged across observers and inducer angles α as a function of SR, task, and eye. The different SRs are depicted in the different panels and decrease from left to right. The tasks are plotted on the axis: IC = illusory curvature discrimination; LC = local discrimination. Error bars indicate 2 standard errors of the mean derived by nonparametric bootstrap resampling with $n = 2000$ samples.



times yielded a significant interaction between the factors task and eye for all four subjects (Table 3).

DISCUSSION

The experimental logic was based on the finding that the presence of an illusory contour facilitates discrimination performance relative to a situation where discrimination performance must rely exclusively on local information (Ringach & Shapley, 1996). The idea was that in the absence of a neural representation of the illusory contour curvature due to the blind spot, performance levels should equal those of a local orientation discrimination task. That is exactly what our data suggest: The facilitation of performance on the illusory contour task could not be achieved when the curvature traversed the blind spot. We observed a selective drop in illusory curvature discrimination performance when the majority of the illusory contour traversed the blind spot of one eye and the other eye was occluded. The observed increase in discrimination thresholds and loss in sensitivity were accompanied by increased response latencies, and thus, were not due to a speed-accuracy tradeoff. The perceptual impairment was specific to illusory contours traversing the blind spot and was not due to the eccentricity of the stimulus. At the same eccentricity, discrimination of illusory contour curvature

was markedly better when the fellow eye was used. The blind spot also specifically interfered with the perception of illusory contours because sensitivity was preserved on a local control task.

We distinguish between two processes involved in the current task: (i) processes involved in representing the illusory contour by means of an activity pattern in a neural population, and (ii) processes involved in “reading out” or discriminating convex and concave curvature. Although the former might allow the mapping of quantitative differences in the amount of curvature, the latter process maps different degrees of curvature into either of the two categories “concave” and “convex.” We attribute the impaired curvature discrimination performance observed here to the absence of a cortical representation of the illusory contour in the blind spot region rather than to a failure in the curvature readout process. This absence of a cortical representation of the contralateral portion of the visual field corresponding to the blind spot has been reported specifically for V1 (Awater et al., 2005; Tong & Engel, 2001; Horton et al., 1990; Ts’o et al., 1990; Tootell & Hamilton, 1989; Tootell et al., 1988). We therefore conclude that V1 neurons play a critical role in generating the illusory contour representation which served as the basis of curvature discrimination in the current task.

Considering the numerous reports of filling-in the blind spot (e.g., Ramachandran, 1992b), one might

Table 3. Results of Individual Three-way ANOVAs on Reaction Times

	<i>Task</i>		<i>Eye</i>		<i>SR</i>		<i>Task × Eye</i>		<i>Task × SR</i>		<i>Eye × SR</i>	
	<i>F</i>	<i>p</i>	<i>F</i>	<i>p</i>	<i>F</i>	<i>p</i>	<i>F</i>	<i>p</i>	<i>F</i>	<i>p</i>	<i>F</i>	<i>p</i>
M. M.	31.83	<.001	14.07	<.001	37.35	<.001	70.78	<.001	7.81	<.001	6.08	.003
#1	28.40	<.001	37.22	<.001	3.46	.033	9.44	.002	5.29	.005	4.54	.012
#2	63.12	<.001					93.68	<.001				
#3			167.37	<.001	3.12	.046	9.24	.003				

How are the present findings reconciled within the abovementioned model of contour completion (Maertens & Pollmann, 2005; Lee, 2003)? The current data substantiate our claim that V1 neurons are obligatory for an illusory contour representation that gives rise to a crisp boundary percept (Maertens & Pollmann, 2005; Muckli et al., 2005; Lee & Nguyen, 2001; Ramsden et al., 2001; Seghier et al., 2000; Grosf et al., 1993). To take into account the available evidence for the importance of higher level visual areas such as the LOC (Murray et al., 2002, 2004; Stanley & Rubin, 2003; Mendola et al., 1999), we suggest that feedback and intracortical signals act in concert to generate an illusory contour representation. However, the present data do not speak to the question of the relative contributions of either intracortical or feedback re-entrant signal propagation because V1 and LOC neurons are lacking their appropriate targets. Instead, we can conclude that although feedback signals might aid the generation of the contour representation in V1, they are not sufficient by themselves. It is the local intracortical signal cascade which is implied to be of major importance. This might be especially true when precise contour judgments are required because intracortical connections link domains of similar orientation preference in V1, whereas feedback from V2 to V1 does not exhibit such specificity (Stettler, Das, Bennett, & Gilbert, 2002).

Acknowledgments

Marianne Maertens was supported by a grant from the Gertrud Reemtsma Foundation. We thank Damian Stanley for his enormous help with an earlier version of this manuscript. We thank F. Bauch, J. Czechowski, C. Kohrs, A. Neubauer, N. Recker, K. Schwiecker, and H. Ulferts for their help with the data collection. We also thank Nava Rubin, Robert Shapley, Nicola Bruno, Richard Ivry, and an anonymous reviewer for helpful discussions and comments on earlier versions of this manuscript.

Reprint requests should be sent to Marianne Maertens, Center for Neural Science, New York University, 4 Washington Place, Room 809, 10003 New York, NY, or via e-mail: marianne.maertens@gmail.com.

REFERENCES

Ahissar, M., & Hochstein, S. (2004). The reverse hierarchy theory of visual perceptual learning. *Trends in Cognitive Sciences*, *8*, 437–464.

Awatramani, H., Kerlin, J. R., Evans, K. K., & Tong, F. (2005). Cortical representation of space around the blind spot. *Journal of Neurophysiology*, *94*, 3314–3324.

Fiorani, M., Rosa, M. G., Gattass, R., & Rocha-Miranda, C. E. (1992). Dynamic surrounds of receptive fields in primate striate cortex: A physiological basis for perceptual completion? *Proceedings of the National Academy of Sciences, U.S.A.*, *89*, 8547–8551.

Flytche, D. H., & Zeki S. (1996). Brain activity related to the perception of illusory contours. *Neuroimage*, *3*, 104–108.

Gold, J. M., Murray, R. F., Bennett, P. J., & Sekuler, A. B. (2000). Deriving behavioural receptive fields for visually completed contours. *Current Biology*, *10*, 663–666.

Grosf, D., Shapley, R., & Hawken, M. (1993). Macaque V1 neurons can signal “illusory” contours. *Nature*, *365*, 550–552.

Grossberg, S., & Mingolla, E. (1985). Neural dynamics of form perception: Boundary completion, illusory figures, and neon color spreading. *Psychological Review*, *92*, 173–211.

Gurnsey, R., Poirier, F. J., & Gascon, E. (1996). There is no evidence that Kanizsa-type subjective contours can be detected in parallel. *Perception*, *25*, 861–874.

Halgren, E., Mendola, J., Chong, C. D., & Dale, A. M. (2003). Cortical activation to illusory shapes as measured with magnetoencephalography. *Neuroimage*, *18*, 1001–1009.

He, S., & Davis, W. L. (2001). Filling-in at the natural blind spot contributes to binocular rivalry. *Vision Research*, *41*, 835–840.

Hirsch, J., DeLaPaz, R., Relkin, N., Victor, J., Kim, K., Li, T., et al. (1995). Illusory contours activate specific regions in human visual cortex: Evidence from functional magnetic resonance imaging. *Proceedings of the National Academy of Sciences, U.S.A.*, *92*, 6469–6473.

Hochstein, S., & Ahissar, M. (2002). View from the top: Hierarchies and reverse hierarchies in the visual system. *Neuron*, *36*, 791–804.

Horton, J. C., Dagi, L. R., McCrane, E. P., & DeMonasterio, F. M. (1990). Arrangement of ocular dominance columns in human visual cortex. *Archives of Ophthalmology*, *108*, 1025–1031.

Hupe, J., James, A., Payne, B., Lomber, S., Girard, P., & Bullier, J. (1998). Cortical feedback improves discrimination between figure and background by V1, V2 and V3 neurons. *Nature*, *394*, 784–787.

Julesz, B. (1971). *Foundations of the cyclopean perception*. Chicago: University of Chicago Press.

Kanizsa, G. (1976). Subjective contours. *Scientific American*, *234*, 48–52.

Kawabata, N. (1983). Global interactions in perceptual completion at the blind spot. *Vision Research*, *23*, 275–279.

Komatsu, H., Kinoshita, M., & Murakami, I. (2002). Neural responses in the primary visual cortex of the monkey during perceptual filling-in at the blind spot. *Neuroscience Research*, *44*, 231–236.

Lee, T., & Nguyen, M. (2001). Dynamics of subjective contour formation in the early visual cortex. *Proceedings of the National Academy of Sciences, U.S.A.*, *98*, 1907–1911.

Lee, T. S. (2003). Computations in the early visual cortex. *Journal of Physiology (Paris)*, *97*, 121–139.

Maertens, M., & Pollmann, S. (2005). fMRI reveals a common neural substrate of illusory and real contours in v1 after perceptual learning. *Journal of Cognitive Neuroscience*, *17*, 1553–1564.

Malach, R., Amir, Y., Harel, M., & Grinvald A. (1993). Relationship between intrinsic connections and functional architecture revealed by optical imaging and in vivo targeted biocytin injections in primate striate cortex. *Proceedings of the National Academy of Sciences, U.S.A.*, *90*, 10469–10473.

Matsumoto, M., & Komatsu, H. (2005). Neural responses in the macaque v1 to bar stimuli with various lengths presented on the blind spot. *Journal of Neurophysiology*, *93*, 2374–2387.

Mendola, J., Dale, A., Fischl, B., Liu, A., & Tootell, R. (1999). The representation of illusory and real contours in human

- cortical visual areas revealed by functional magnetic resonance imaging. *Journal of Neuroscience*, *19*, 8560–8572.
- Muckli, L., Kohler, A., Kriegeskorte, N., & Singer, W. (2005). Primary visual cortex activity along the apparent-motion trace reflects illusory perception. *PLoS Biology*, *3*, e265.
- Murray, M., Foxe, D., Javitt, D., & Foxe, J. (2004). Setting boundaries: Brain dynamics of modal and amodal illusory shape completion in humans. *Journal of Neuroscience*, *24*, 6898–6903.
- Murray, M., Wylie, G., Higgins, B., Javitt, D., Schroeder, C., & Foxe, J. (2002). The spatiotemporal dynamics of illusory contour processing: Combined high-density electrical mapping, source analysis, and functional magnetic resonance imaging. *Journal of Neuroscience*, *22*, 5055–5073.
- Nieder, A. (2002). Seeing more than meets the eye: Processing of illusory contours in animals. *Journal of Comparative Physiology A: Neuroethology, Sensory, Neural, and Behavioral Physiology*, *188*, 249–260.
- Pillow, J., & Rubin, N. (2002). Perceptual completion across the vertical meridian and the role of early visual cortex. *Neuron*, *33*, 805–813.
- Ramachandran, V. S. (1992a). Filling in the blind spot. *Nature*, *356*, 115.
- Ramachandran, V. S. (1992b). Blind spots. *Scientific American*, *266*, 86–91.
- Ramsden, B., Hung, C., & Roe, A. (2001). Real and illusory contour processing in area V1 of the primate: A cortical balancing act. *Cerebral Cortex*, *11*, 648–665.
- Ringach, D., & Shapley, R. (1996). Spatial and temporal properties of illusory contours and amodal boundary completion. *Vision Research*, *36*, 3037–3050.
- Ritzl, A., Marshall, J., Weiss, P., Zafiris, O., Shah, N., Zilles, K., et al. (2003). Functional anatomy and differential time courses of neural processing for explicit, inferred, and illusory contours. An event-related fMRI study. *Neuroimage*, *19*, 1567–1577.
- Rubin, N., Nakayama, K., & Shapley, R. (1997). Abrupt learning and retinal size specificity in illusory-contour perception. *Current Biology*, *7*, 461–467.
- Seghier, M., Dojat, M., Delon-Martin, C., Rubin, C., Warnking, J., Segebarth, C., et al. (2000). Moving illusory contours activate primary visual cortex: An fMRI study. *Cerebral Cortex*, *10*, 663–670.
- Shiple, T., & Kellman, P. (1992). Strength of visual interpolation depends on the ratio of physically specified to total edge length. *Perception & Psychophysics*, *52*, 97–106.
- Smith, A., Singh, K., Williams, A., & Greenlee, M. (2001). Estimating receptive field size from fMRI data in human striate and extrastriate visual cortex. *Cerebral Cortex*, *11*, 1182–1190.
- Stanley, D., & Rubin, N. (2005). Rapid detection of salient regions: Evidence from apparent motion. *Journal of Vision*, *5*, 690–701.
- Stanley, D., & Rubin, N. (2003). fMRI activation in response to illusory contours and salient regions in the human lateral occipital complex. *Neuron*, *37*, 323–331.
- Stettler, D., Das, A., Bennett, J., & Gilbert, C. (2002). Lateral connectivity and contextual interactions in macaque primary visual cortex. *Neuron*, *36*, 739–750.
- Tong, F., & Engel, S. (2001). Interocular rivalry revealed in the human cortical blind-spot representation. *Nature*, *411*, 195–199.
- Tootell, R., & Hamilton, S. (1989). Functional anatomy of the second visual area (V2) in the macaque. *Journal of Neuroscience*, *9*, 2620–2644.
- Tootell, R. B., Hadjikhani, N. K., Vanduffel, W., Liu, A. K., Mendola, J. D., Sereno, M. I., et al. (1998). Functional analysis of primary visual cortex (V1) in humans. *Proceedings of the National Academy of Sciences, U.S.A.*, *95*, 811–817.
- Tootell, R. B., Switkes, E., Silverman, M. S., & Hamilton, S. L. (1988). Functional anatomy of macaque striate cortex: II. Retinotopic organization. *Journal of Neuroscience*, *8*, 1531–1568.
- Tripathy, S. P., Levi, D. M., & Ogmen, H. (1996). Two-dot alignment across the physiological blind spot. *Vision Research*, *36*, 1585–1596.
- Ts'o, D., Frostig, R., Lieke, E., & Grinvald, A. (1990). Functional organization of primate visual cortex revealed by high resolution optical imaging. *Science*, *249*, 417–420.
- von der Heydt, R., Peterhans, E., & Baumgartner, G. (1984). Illusory contours and cortical neuron responses. *Science*, *224*, 1260–1262.
- Wichmann, F. A., & Hill, N. J. (2001a). The psychometric function: I. Fitting, sampling, and goodness of fit. *Perception & Psychophysics*, *63*, 1293–1313.
- Wichmann, F. A., & Hill, N. J. (2001b). The psychometric function: II. Bootstrap-based confidence intervals and sampling. *Perception & Psychophysics*, *63*, 1314–1329.
- Wolf, E., & Gardiner, J. S. (1963). Sensitivity of the retinal area in one eye corresponding to the blind spot in the other eye. *Journal of the Optical Society of America*, *53*, 1437–1445.
- Yoshino, A., Kawamoto, M., Yoshida, T., Kobayashi, N., Shigemura, J., Takahashi, Y., et al. (2006). Activation time course of responses to illusory contours and salient region: A high-density electrical mapping comparison. *Brain Research*, *1071*, 137–144.